Macromolecular Research, Vol. 11, No. 6, pp 418-424 (2003)

Poly(methyl methacrylate-*co*-styrene)/Silicate Nanocomposites Synthesized by Multistep Emulsion Polymerization

Yeong Suk Choi, Yoon Kyung Kim, and In Jae Chung*

Department of Chemical and Biomolecular Engineering, Korea Advanced Institute of Science and Technology, 373-1, Guseong-dong, Yuseong-gu, Daejeon 305-701, Korea

Received Mar. 3, 2003; Revised Sept. 5, 2003

Abstract: Exfoliated poly(methyl methacrylate-*co*-styrene) [P(MMA-*co*-ST)]/silicate nanocomposites were synthesized through a multistep emulsion polymerization. The methyl methacrylate monomers were polymerized first and then the styrene monomers were polymerized. The nanocomposites had core-shell structures consisting of PMMA (core) and PS (shell); these structures were confirmed by ^{1}H NMR spectroscopy and TEM, respectively. P(MMA-*co*-ST) copolymers showed two molecular weight profiles and two glass transition temperatures (T_g) in GPC and DMA measurements. At 30 °C, the nanocomposites exhibited 83 and 91% increases in their storage moduli relative to the neat copolymer because the silicate layers were dispersed uniformly in the polymer matrix.

Keywords: poly(methyl methacrylate-*co*-styrene), core-shell structures, silicate, nanocomposite, emulsion polymerization.

Introduction

Core-shell structured materials[1-14,31-33] show high impact strength and improved toughness, so they have potential applications for high value-added materials such as membrane separations in biotechnology or spacers in liquid crystal displays. Lots of works have been performed to obtain particles with well designed morphology, usually prepared by seeded emulsion polymerization techniques.[8-16] It is a general view that thermodynamic and kinetic factors affect formation of the morphology in particles.[12,15,16] Researches on core-shell structure in polymer/silicate nanocomposites[17-20,24-27,34,35] were rare, since high aspect ratio of silicate layers may hinder the formation of the structure, but the addition and the exfoliation of silicate layers will enhance mechanical properties of the polymer/silicate nanocomposites.

Among commercial polymers, poly(methyl methacrylate) (PMMA) and polystyrene (PS) are chosen as matrixes, because they have merits and demerits, which are compensated with each other. PMMA[19,25] has excellent transparence and high modulus, but its melt viscosity is too high for melt processing. While PS[18-20] can be produced in various shapes by melt processing, but it has relatively low modulus. Blending PMMA and PS will not be a good method for the desired morphology in the composite, since the two polymers are immiscible. So the core-shell structured polymer will be an elusive method for the purpose. To obtain the core-shell structure, the composite is designed to have core PMMA with exfoliated silicate layers and shell PS.

In this article, the exfoliated core-shell structured polymer/silicate nanocomposites are produced by a multistep emulsion polymerization, which involves two procedures: 1) the delamination of pristine clays, and 2) the formation of the core-shell structure of PMMA and PS. The delamination of silicates is obtained by the polymerization of MMA, because PMMA exfoliated the silicate layers during its polymerization with a reactive surfactant,[25-27] and then styrene monomer was supplied continuously to the reactor to make the shell of PS. The morphology and mechanical properties of the nanocomposites are measured.

Experimental

Materials. Sodium montmorillonite (Na-MMT: Kunipia-F) with a cation exchange capacity (CEC) of 119 mequiv/100 g was provided by Kunimine co. and dispersed in deionized water for 24 hrs at ambient temperature before use. MMA, styrene, 2-acrylamido-2-methyl-1-propanesulfonic acid (AMPS),[21-23] and dodecylbenzenesulfonic acid sodium salt (DBS-Na) were purchased from Aldrich Chemical and used as received without further purifications. A free radical initiator, potassium persulfate (KPS), was obtained from Junsei and recrystallized in deionized water. Tetrahydrofuran (THF) of HPLC solvent grade (Merk) was used as received for polymer recovery in extraction and reverse ion exchange

*e-mail: chung@kaist.ac.kr

procedure. *N*-Hexane (Junsei), a nonsolvent for copolymers was distilled under a normal pressure. Lithium chloride (LiCl, Junsei) for the reverse ion exchange was recrystallized with THF. Acetone and isopropyl alcohol (Merk) of HPLC solvent grades were used as received for selective extraction of core polymers.

Synthesis of Core-Shell Structured P(MMA-*co*-ST)/Silicate Nanocomposites.

First Stage: Various amounts of Na-MMT water dispersions, 5 g of MMA, 0.3 g of AMPS, 10 g of DBS-Na solution (DBS-Na/water = 5 g/45 g), and 15 g of initiator solution (KPS/water = 1 g/99 g) were charged into a 1 L four-neck reactor equipped with a baffle stirrer, a reflux condenser, a nitrogen inlet, and a rubber septum. Deionized water was added to the reactor, so that the total weight of mixture was 500 g. The reactor was stirred at 200 rpm for 1 hr under nitrogen gas at an ambient temperature. Then, the temperature of the reactor was raised to 75 °C and kept for 1 hr.

Second Stage: After the first stage of polymerization, 45 g of MMA was continuously fed into the reactor at a rate of 0.2 cc/min using a syringe pump. When MMA feeding was finished, 5 g of DBS-Na solution (10 wt% of aqueous solution) was injected through a septum and the temperature was raised to 95 °C. Then, 50 g of styrene was charged with the same feed rate of MMA. During the entire polymerization, we maintained the concentration of DBS-Na low to avoid secondary nucleation by new soap micelles, and the polymerization was performed under monomer starvation conditions, that is, the feed rate of monomers was lower than the polymerization rate of the system. After the monomer feeding was completed, the reactor was stirred for additional 1 hr at 95 °C to polymerize residual monomers. P(MMA-*co*-ST)/silicate nanocomposites were separated by freeze-drying for 5 days and further dried under a high vacuum at 100 °C for 1 day.

Polymer Recovery. To measure molecular weights and ^{1}H NMR spectra, the copolymers were retrieved from the nanocomposites in the following way.[25-27] For example, 0.1 g of freeze-dried nanocomposite was dispersed in 80 mL of THF for 2 hrs to which LiCl of 0.3 g was added and stirred for 5 days at an ambient temperature. This procedure was called a reverse ion exchange. The mixture was centrifuged to separate the polymer from the silicate cake at 6,000 rpm for 30 min. The filtered solution was viscous and transparent. The solution was filtered with a 0.45 μm membrane filter to remove clays or unwanted particles and poured into *n*-hexane (10-20 folds) to precipitate the copolymer. The precipitated copolymer was filtered and dried in a high vacuum at 100 °C for 50 hrs. The copolymer was subjected to measurements of GPC and NMR.

Extraction Core Polymers with a Mixed Solvent.[31] The interfacial area between core PMMA and shell PS might have some portion of random copolymers, because small amount of MMA would still exist when styrene shell monomer was added into the reactor. To determine the portion of random copolymers in the samples, core polymers were selectively extracted with a mixture of acetone/isopropyl alcohol (90 g/10 g) at a sample concentration less than 1.5% by weight. The mixture of sample and solvent was stirred magnetically for more than 72 hrs at a room temperature. The transparent solution in the mixture was decanted and centrifuged to remove insoluble parts such PS or silicate layers. The extract was filtered with a 0.45 μm membrane filter and poured into *n*-hexane (10-20 folds) to precipitate polymer. The precipitated polymer was dried under high vacuum. PMMA/PS composition and molecular weights of the precipitated polymer were determined using ^{1}H NMR and GPC.

Characterization. All mechanical properties of the composites were measured without further treatments after the drying procedure except X-ray measurements. X-ray diffraction patterns of the composites were obtained by using a Rigaku Xray generator (CuKα with $\lambda = 0.154$ nm) with a scanning rate of 2°/min in a 2θ range of 1.2-10° at an ambient temperature. Oligomers or surfactants, which tend to enlarge the basal space of silicates, may exist in the spaces between silicate layers. With these impurities, the X-ray diffraction patterns of the nanocomposites will not provide correct information on the gap sizes between silicate layers in polymer matrix. To remove the impurities from the composites, small amounts of final composites were extracted by a Soxhlet extractor for 12 hrs with THF and dried under a highly reduced pressure at 100 °C for 50 hrs. The extracted composites were molded in disk shapes before XRD measurements.

Molecular weights of copolymers obtained by the recovery procedure in the previous section were measured by using a Waters GPC system equipped with six styragel HR columns (two 500, two 10^3, 10^4, and 10^5) and a Water 410 RID detector at a flow rate of THF 2.0 mL/min at a room temperature after the calibration with 5 standard polystyrene samples.

Thermogravimetric analyses (TGA) were carried out with a Perkin-Elmer thermobalance by heating samples from room temperature to 600 °C with a rate of 10 °C/min under a N_2 atmosphere.

^{1}H NMR spectra were recorded on a Bruker DMX 600 spectrometer employing THF as a solvent.

Storage moduli (E') and tan δ were obtained by a Rheometric Scientific DMTA4 using a dual cantilever bending mode from 30 to 170 °C with a heating rate of 4 °C/min under 0.01% of deformation at 1 Hz of frequency. Samples were molded in $10 \times 20 \times 1.3$ mm size at 170 °C for 4 min under 3,000 psi of pressure. Glass transition temperatures, T_g, were determined by maximum peak in the tan δ vs. temperature scan.

The morphologys of nanocomposites were examined by a Philips CM-20 transmission electron microscope (TEM). The samples were cut into slices of about 100 nm thickness

with a microtom system, and loaded on a copper grid coated with carbon. PS was stained selectively with RuO_4. The stained sections were observed by using the TEM with accelerating voltage of 160 kV.

Results and Discussion

In the name of sample, M stands for the monomer, MMA, S for styrene, A for AMPS, T for pristine silicate, Na-MMT, and the numbers following M and S indicate the weight of monomers in the composites. The number after T indicates the relative weight percentage of the silicate to the weight of monomers charged.

Figure 1 shows the X-ray diffraction patterns taken from AM50S50 series after THF extraction for 12 hrs. Basal spacing, d_{001}, of silicate layers is calculated from the peak position by using the Braggs law. The basal spacing of the pristine silicate is 1.14 nm. In these nanocomposites, no peak is observed, which means that silicate layers are exfoliated in polymer matrix during polymerization.

Figure 2(a) represents ^{1}H NMR spectrum of the copolymer extracted from AM50S50T3% with THF. Solvent peak, THF, is shown at 3.58 δ. Phenyl protons of PS are observable in the range of 6.4-7.1 δ. Methylene and methine protons of PS are found at 1.5 and 1.8 δ, respectively. Methoxy protons of PMMA occur at 3.8 δ, methylene protons occur at 2.7-1.9 δ and methyl protons at 1.24 δ (isotactic), 1.04 δ (hetero), and 0.8 δ (syndiotactic). Those are the characteristic peaks of homo-PS and homo-PMMA observed in ^{1}H NMR spectra. These sharp tacticity peaks from methyl protons of PMMA can not be observed in random copolymers of PS and PMMA because of peak overlapping.[30] The tacticity of PMMA obtained from Figure 2(a) is similar to that of homo-PMMA reported by Alexandre Blumstein *et al.*[28,29] The peak areas of methyl protons in PMMA and phenyl protons in PS show the one-to-one ratio which is the same ratio of monomers.

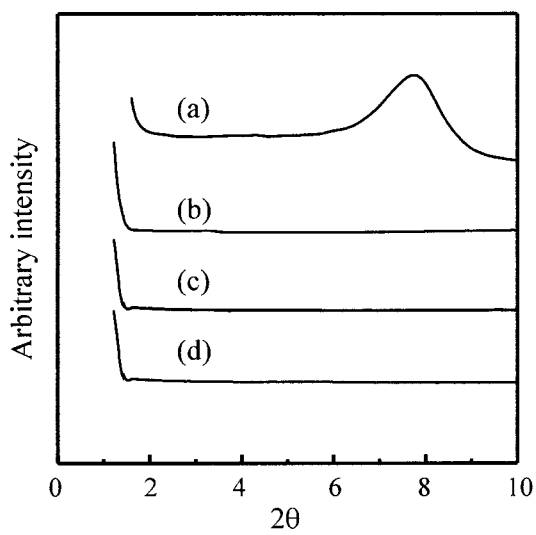

Figure 1. X-ray diffraction patterns of (a) pristine silicate, Na-MMT, given as a reference, (b) AM50S50T1%, (c) AM50S50T3%, and (d) AM50S50T5% extracted with THF for 12 hrs with a Soxhlet extraction apparatus, and compressed in a disk shape.

On the other hand, if considerable amount of core monomer (MMA) exists in emulsion particles, shell monomer (styrene) addition will cause random copolymerization that deters formation of the core-shell structure. Figure 2(b) shows the ^{1}H NMR spectra of core polymers extracted with acetone and isopropyl alcohol. The ratios of PMMA and PS in core polymers are determined with the phenyl proton peak areas of PS (at 6.4-7.1 δ) and the methyl proton peak areas of PMMA (at 0.8, 1.04, 1.24 δ). The ratios of PMMA/PS in core polymers are 6.2/1 for AM50S50T0%, 10/1 for AM50S50T1%, 38.9/1 AM50S50T3%, and 8.9/1 AM50S50T5%. The core polymers mainly consist of PMMA, because there is a strong interaction between hydrophilic silicate layers and PMMA. The possibility of random copolymerization in core-shell interfacial areas may be low, because the ^{1}H NMR spectra in Figure 2(b) sustain the characteristic tacticity peaks of PMMA.

Because PMMA is more hydrophilic than shell PS, core PMMA tends to move toward the surface of a particle forming inverted core-shell structure or hemisphere structure.[9,11,33] TEM image in Figure 3 shows the structure of core-shell. In Figure 3(a), the dark and bright portions are assigned as shell PS and core PMMA, respectively. In Figure 3(b), dark strips indicating silicate layers intersect a bright particle. The shape of copolymer around the silicate layer is ellipsoidal. The high aspect ratio of silicate layer may hinder the formation of a spherical shape. It seems that, after the silicate layer is delaminated from the primary silicate particle by the polymerization of MMA, the silicate layer is surrounded by PMMA and the polymerization continues on the layer surface as monomers are charged.

Molecular weights of entire copolymers and core polymers extracted from nanocomposites are shown in Table I and Figure 4, respectively. In Figure 4(a), the profiles show two peaks and the polydispersity indices (PDI) are broad. It means that the core-shell structured copolymers might be synthesized by at least two different polymerization environments. To identify each peak in Figure 4(a), molecular weights of the core polymers are measured with GPC. The molecular weights in Figure 4(b) show the same values as the lower molecular weight peak in Figure 4(a), and it indicates that the lower molecular weight portion is mainly core PMMA.

Figure 5 shows storage moduli of synthesized core-shell structured P(MMA-*co*-ST)/silicate nanocomposites. The storage moduli appear higher uniformly along the temperature as the content of silicate increases. Glass transition temperatures, T_g, are obtained from the maximum peak temperatures of tan δ in Figure 6. The nanocomposites and

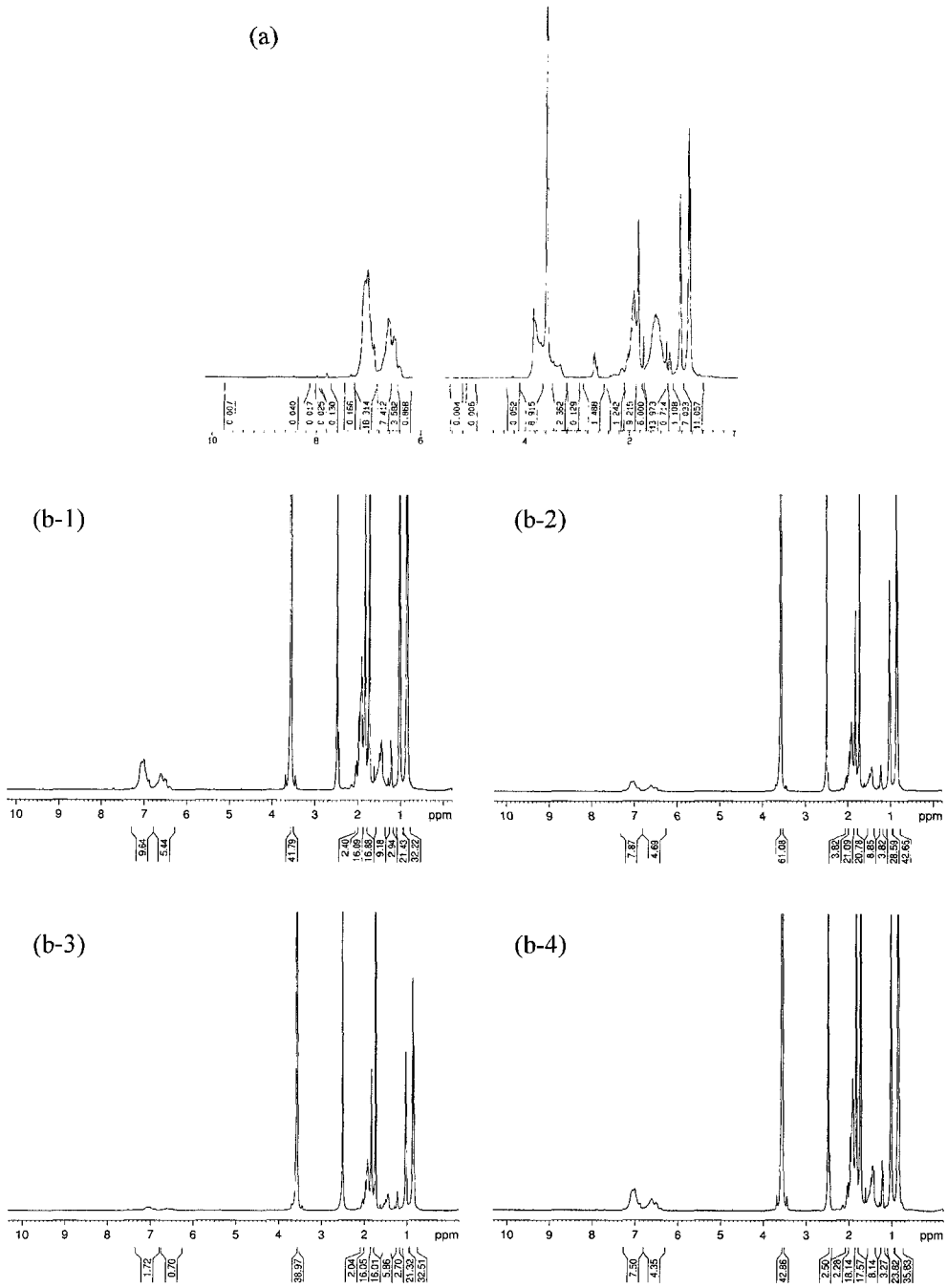

Figure 2. ^{1}H NMR spectrum of (a) copolymer recovered entirely from AM50S50T3% by extraction with THF. ^{1}H NMR spectra of (b) core polymers extracted selectively with acetone and isopropyl alcohol: (b-1) AM50S50T0%, (b-2) AM50S50T1%, (b-3) AM50S50T3%, and (b-4) AM50S50T5%. THF was used as a solvent without TMS.

the neat copolymer show two glass transition temperatures. The lower peak at about 130 °C is the glass transition temperature of PS and the higher peak at about 150 °C is the glass transition temperature of PMMA. The double glass transition temperatures indicate that the segmental motion of PMMA does not interrupt that of PS. If MMA and styrene were polymerized randomly, a single glass transition would be observed.

The thermal decomposition behaviors of nanocomposites are given in Figure 7. Onset temperature of thermal degradation for AM50S50T0% appears at 329 °C. AM50S50T1% and AM50S50T3% show the degradation temperature at 350 °C. AM50S50T5% begins to degrade thermally at 360 °C. The onset points shift to higher temperatures as the

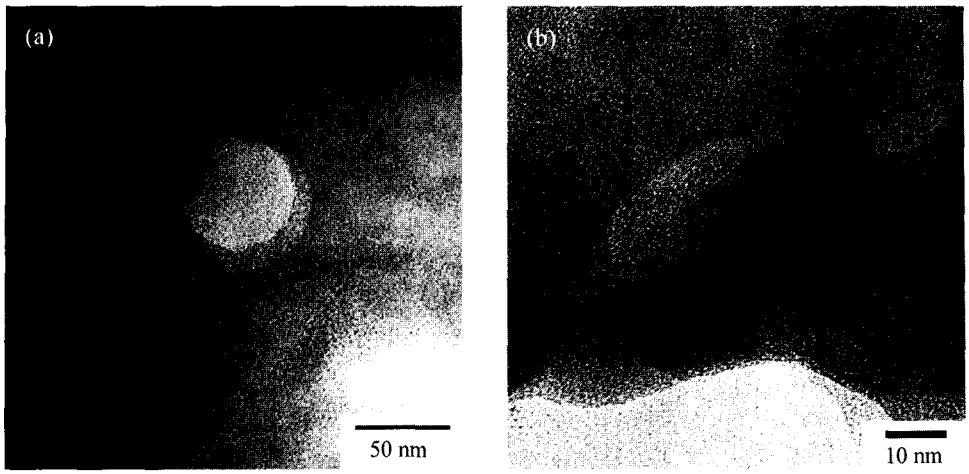

Figure 3. TEM micrographs of (a) AM50S50T0% and (b) AM50S50T3%.

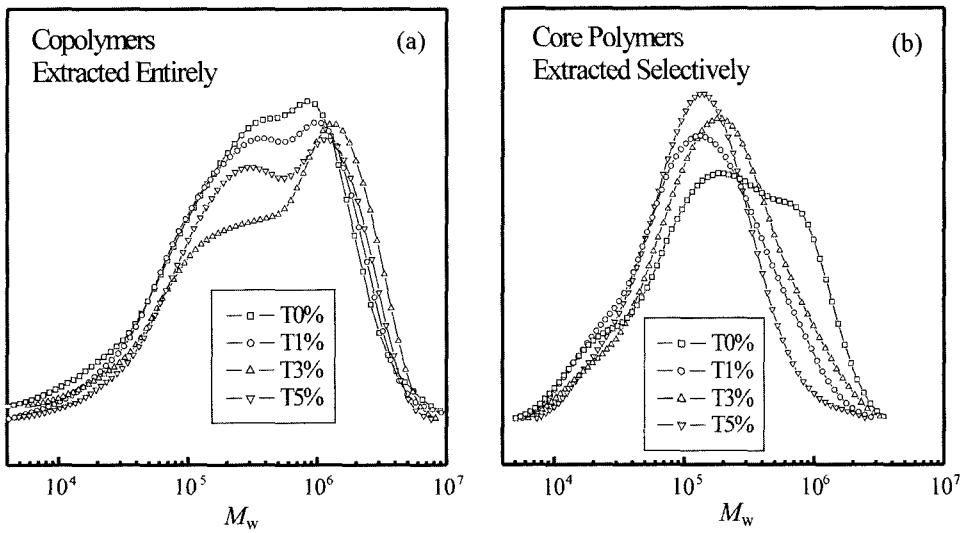

Figure 4. GPC profiles of (a) copolymers, P(MMA-*co*-ST), recovered entirely from AM50S50 series with THF and (b) core polymers extracted selectively from AM50S50 series with acetone and isopropyl alcohol.

Table I. Molecular Weights of (a) Copolymers, P(MMA-*co*-ST), Recovered Entirely from AM50S50 Series with THF and (b) Core Polymers Extracted Selectively from AM50S50 Series with Acetone and Isopropyl Alcohol

(a) Copolymers Extracted Entirely	M_n	M_w	PDI
AM50S50T0%	82,000	71,000	8.67
AM50S50T1%	119,000	739,000	6.17
AM50S50T3%	116,000	911,000	7.85
AM50S50T5%	141,000	783,000	5.52
(b) Core Polymers Extracted Selectively	M_n	M_w	PDI
AM50S50T0%	79,000	378,000	4.78
AM50S50T1%	68,000	228,000	3.35
AM50S50T3%	87,000	291,000	3.34
AM50S50T5%	77,000	189,000	2.45

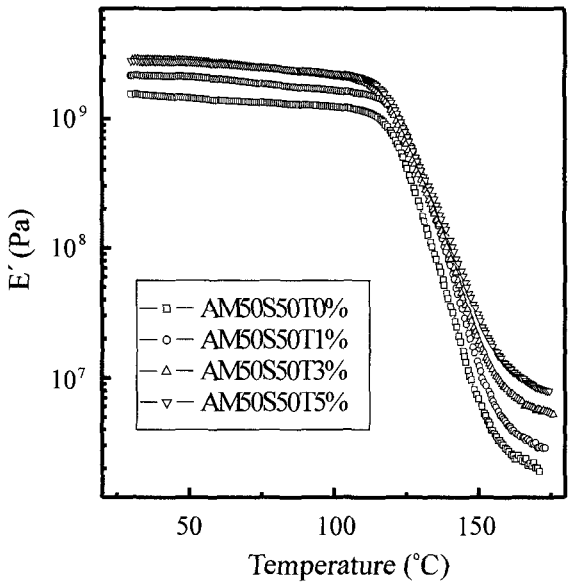

Figure 5. Dependence of storage modulus of AM50S50 series on temperature with DMA scans.

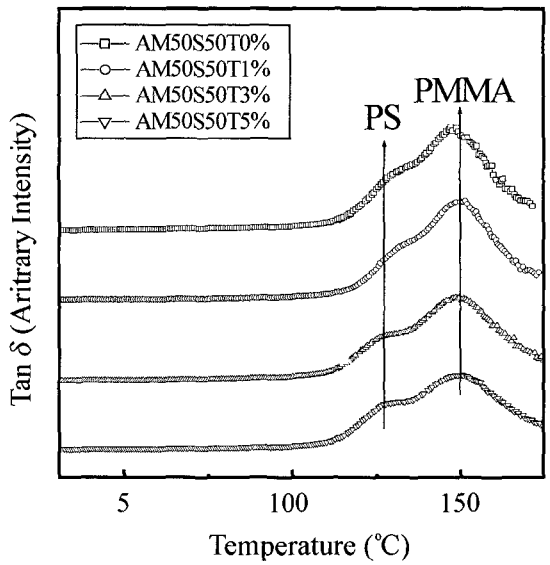

Figure 6. Tan δ of AM50S50 series on temperature with DMA scans.

content of silicate increases. The weight losses by main chain thermal degradation occur around 350-450 °C.

Conclusions

Exfoliated core-shell structured P(MMA-*co*-ST)/silicate nanocomposites were obtained by a sequential emulsion polymerization. The characteristic tacticity peaks of PMMA and PS explained that the core-shell structures were synthesized in P(MMA-*co*-ST)/silicate nanocomposites. The morphology of core-shell structure and the exfoliated state of silicate layers could be confirmed by TEM images. The nanocomposites showed 86 and 91% increase in storage modulus at 30 °C when compared to the neat copolymer. The nanocomposites and neat copolymer had two glass transition temperatures showing at 130 °C for the PS segmental motion and at 150 °C for the PMMA molecular motion. Two glass transition temperatures and GPC profiles might result from the core-shell structure of copolymers.

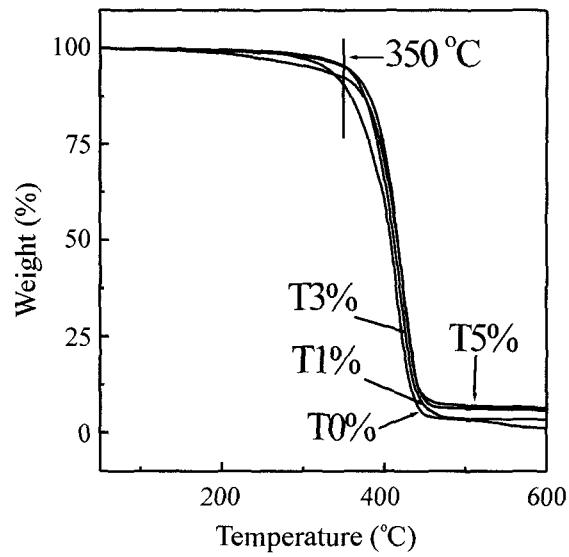

Figure 7. Thermal gravimetric curves for AM50S50 series under N_2 atmosphere.

Acknowledgements. The authors express their sincere thanks to KOSEF (Korea Science and Engineering Foundation) and CAFPoly (Center for Advanced Functional Polymers) for their financial support.

References

(1) M. Schneider, T. Pith, and M. Lambla, *Polym. Adv. Technol.*, **7**, 425 (1996).
(2) I. Luzinov, A. Voronov, S. Minko, R. Kraus, W. Wilke, and A. Zhuk, *J. Appl. Polym. Sci.*, **61**, 1101 (1996).
(3) F. Caruso, A. S. Susha, M. Giersig, and H. Möhwald, *Adv. Mater.*, **11**, 950 (1999).
(4) I. Pastoriza-Santos, D. S. Koktysh, A. A. Mamedov, M. Giersig, N. A. Kotov, and M. Liz-Marzán, *Langmuir*, **16**, 2731 (2000).
(5) Q. Kalinina and E. Kumacheva, *Chem. Mater.*, **13**, 35 (2001).
(6) Q. Kalinina and E. Kumacheva, *Macromolecules*, **35**, 3675 (2002).
(7) D. Gan and A. Lyon, *J. Am. Chem. Soc.*, **123**, 8203 (2001).
(8) M. Okubo, H. Ahmad, and M. Komura, *Coll. Polym. Sci.*,

274, 1188 (1996).
(9) Y. C. Chen, V. Dimonie, and M. S. ElAasser, *Macromolecules*, **24**, 3779 (1991).
(10) P. Marion, G. Beinert, D. Juhue, and J. Lang, *Macromolecules*, **30**, 123 (1997).
(11) K. Landfester, C. Boeffel, M. Lambla, and H. W. Spiess, *Macromolecules*, **29**, 5972 (1996).
(12) N. Dingenouts, Ch. Norhausen, and M. Ballauff, *Macromolecules*, **31**, 8912 (1998).
(13) S. Kirsch, A. Doerk, E. Bartsch, and H. Sillescu, *Macromolecules*, **32**, 4508 (1999).
(14) J. E. Jönsson, O. J. Karlsson, H. Hassander, and B. Törnell, *Macromolecules*, **34**, 1512 (2001).
(15) H. A. S. Schoonbrood, A. L. German, and R. G. Gilbert, *Macromolecules*, **28**, 34 (1995).
(16) C. Plessis, G. Arzamendi, J. R. Leiza, H. A. S. Schoonbrood, D. Charmot, and J. M. Asua, *Macromolecules*, **34**, 5147 (2001).
(17) G. D. Kim, D. H. Lee, B. Hoffmann, J. Kressler, and G. Stöppelmann, *Polymer*, **42**, 1095 (2001).
(18) M. W. Noh and D. C. Lee, *Polym. Bull.*, **42**, 619 (1999).
(19) M. Okamoto, S. Morita, H. Taguchi, Y. H. Kim, T. Kotaka, and H. Tateyama, *Polymer*, **41**, 3887 (2000).
(20) B. Hoffmann, C. Dietrich, R. Thomann, C. Friedrich, and R. Mülhaupt, *Macromol. Rapid Commun.*, **21**, 57 (2000).
(21) M. Seki, Y. Morishima, and M. Kamachi, *Macromolecules*, **25**, 6540 (1992).
(22) Y. Morishima, S. Nomura, T. Ikeda, M. Seki, and M. Kamachi, *Macromolecules*, **28**, 2874 (1995).
(23) H. Aota, S. I. Akaki, Y. Morishima, and M. Kamachi, *Macromolecules*, **30**, 4090 (1997).
(24) H. Y. Byun, M. H. Choi, and I. J. Chung, *Chem. Mater.*, **13**, 4221 (2001).
(25) Y. S. Choi, M. H. Choi, K. H. Wang, S. O. Kim, Y. K. Kim, and I. J. Chung, *Macromolecules*, **34**, 8978 (2001).
(26) Y. S. Choi, K. H. Wang, M. Xu, and I. J. Chung, *Chem. Mater.*, **14**, 2936 (2002).
(27) Y. K. Kim, Y. S. Choi, K. H. Wang, and I. J. Chung, *Chem. Mater.*, **14**, 4990 (2002).
(28) A. Blumstein, S. L. Malhotra, and A. C. Watterson, *J. Polym. Sci., Polym. Phys.*, **8**, 1599 (1970).
(29) A. Blumstein, K. K. Parikh, S. L. Malhotra, and R. Blumstein, *J. Polym. Sci., Polym. Phys.*, **9**, 1681 (1971).
(30) S. A. Heffner, F. A. Bovey, L. A. Verge, P. A. Mirau, and A. E. Toneli, *Macromolecules*, **19**, 1628 (1986).
(31) S. Shen, M. S. ElAasser, V. L. Dimonie, J. W. Vanderhoff, and E. D. Sudol, *J. Polym. Sci., Part A: Polym. Chem.*, **29**, 857 (1991).
(32) D. I. Lee and T. Ishikawa, *J. Polym. Sci., Polym. Chem. Ed.*, **21**, 147 (1983).
(33) D. R. Stutman, A. Klolin, M. S. ElAasser, and J. W.Vanderhoff, *Ind. Eng. Chem. Prod. Res. Dev.*, **24**, 404 (1985).
(34) J. G. Ryu, J. W. Lee, and H. Kim, *Macromol. Res.*, **10**, 187 (2002).
(35) N.G. Sahoo, C. K. Das, A. B. Panda, and P. Pramanik, *Macromol. Res.*, **10**, 369 (2002).